

Direct Evidence for the Spatial Correlation between Individual Particle Traversals and Localized CDKN1A (p21) Response Induced by High-LET Radiation

M. Scholz,^{a,b,1} B. Jakob^a and G. Taucher-Scholz^a

^a *Gesellschaft für Schwerionenforschung (GSI)/Biophysik, Planckstrasse 1, D-64291 Darmstadt, Germany; and* ^b *Radiologische Klinik der Universität Heidelberg, In Neuenheimer Feld 400, D-69120 Heidelberg, Germany*

Scholz, M., Jakob, B. and Taucher-Scholz, G. Direct Evidence for the Spatial Correlation between Individual Particle Traversals and Localized CDKN1A (p21) Response Induced by High-LET Radiation. *Radiat. Res.* 156, 558–563 (2001).

The spatial correlation between individual particle traversals and the nuclear CDKN1A (p21) response after high-LET irradiation of human fibroblasts was investigated. The experiments were based on a technique for the retrospective detection of particle traversals by means of nuclear track detectors, which were used as the cell substratum. This technique requires the precise repositioning of a sample at different steps of the experimental procedure and uses a computerized microscope stage control. The precision of the spatial correlation is further enhanced by means of reference marks in the track etch material that are produced by preirradiation of the plates with charged-particle beams at low fluences. The pattern of the CDKN1A foci that were induced by charged-particle traversals at 1 h postirradiation was found to coincide extremely well with the pattern of particle tracks. This represents direct evidence that CDKN1A foci are located at the sites of particle traversals and thus provides further evidence that the radiation-induced accumulation of the CDKN1A protein takes place at the sites of the primary damage. © 2001 by Radiation Research Society

INTRODUCTION

In a recent study, we showed that heavy-ion irradiation of human fibroblasts led to an extremely localized nuclear response of the CDKN1A protein (formerly known as p21 or WAF1) (*1*). The number of CDKN1A foci per cell nucleus after heavy-ion irradiation suggested a direct correlation with the number of particle traversals and therefore a spatial correlation between foci and particle traversals.

¹ Author to whom correspondence should be addressed at GSI/Biophysik, Planckstrasse 1, D-64291 Darmstadt, Germany; e-mail: m.scholz@gsi.de.

However, this conclusion was based on statistical arguments, comparing the number of foci with the average number of particle hits that are expected at a given fluence and geometrical size of the nucleus. The assignment of individual foci to the sites of individual particle traversals remained to be proven.

In principle, using a microbeam facility, where the locations of individual particle traversals can be predefined, would be ideal for such investigations. However, alternative approaches have been used which also allow the determination of the intranuclear location of particle traversals through a cell with sufficient precision, but with somewhat less technical effort (*2–4*). These methods are based on a retrospective detection of traversals in the nuclear track detection material on which the cells are grown.

In this paper, we describe the adaptation of such a method to our special needs and its application to analyze the spatial correlation of CDKN1A foci and charged-particle traversals.

MATERIALS AND METHODS

Our approach is similar to the method proposed by Soyland and Hassfjell (*2, 3*). The procedure of fluorescence imaging and track image matching includes the following general steps, which are explained in more detail below:

1. Cells are grown on CR39 plastic material, which is used as a nuclear track detector. Individual particle tracks can be made visible in this material by etching in NaOH.
2. Cells are irradiated and immunostained using a CDKN1A antibody as described previously (*1*).
3. Images of the nuclei showing CDKN1A foci are taken (denoted as image type I in the following), and the positions of the cells are stored using a computerized microscope stage control. At the same time, phase-contrast images are taken at the same position (denoted as image type II).
4. After the images of CDKN1A foci are taken, cells are removed from the CR39 plates, and the plates are etched for track detection.
5. The plate positions for which images of CDKN1A foci were taken are relocated, and images are taken at the same position to show the pattern of particle traversals (denoted as image type III).

6. By comparing the different images, the spatial correlation of tracks and foci is determined. Possible displacements due to inaccuracies in repositioning can be detected by means of reference tracks, which had been produced by preirradiation of the CR39 with charged particles.

Cell Culture

Normal human foreskin fibroblasts (AG15022B, Coriell Cell Repository, Camden, NJ; 25–30 cumulated population doublings, passage 12–13) were grown on CR39 plates (2 × 2 cm², 1 mm thick; Pershore Mouldings Ltd., Pershore, England; for the details of preparation of the CR39 plates, see below). Cells were incubated at 37°C and 100% humidity in 95% air/5% CO₂ in Eagle's MEM (PAN Systems, Aidenbach, Germany) containing 1% glutamine, 0.5% penicillin/streptomycin, and 10% fetal calf serum. To improve the attachment and growth of the fibroblasts on the CR39 material, it was coated with CELL-TAK (Collaborative Biomedical Products, Bedford, MA). Cells were grown to a subconfluent density of approximately 30,000 cells cm⁻².

Irradiation

CR39 plates were fixed in 35-mm Petri dishes to allow the use of the standard irradiation procedure at the low-energy beam line of the UNILAC at GSI Darmstadt (5). Cells on CR39 plates were irradiated with 10.1 MeV/nucleon calcium ions at a fluence of 2 × 10⁶ particles cm⁻² (LET 1370 keV/μm). Irradiation of a sample typically lasted about 15–30 s; the fluence was determined by means of nuclear track detectors, with an error smaller than 10%.

Immunostaining

Immunostaining of CDKN1A (p21) was performed according to the protocol described previously (1) using a Cip1 (CDKN1A) monoclonal antibody (Transduction Laboratories) and a fluorescence-labeled secondary antibody [Alexa 488 goat anti-mouse IgG F(ab')₂ fragment conjugate, Molecular Probes]. The samples were prepared after 1 h postirradiation incubation at 37°C in 95% air/5% CO₂ to allow sufficient accumulation of protein for an optimal signal.

Etching of CR39 Material

Latent tracks obtained by charged-particle irradiation were developed by etching the CR39 plates in 11 mol liter⁻¹ NaOH at 85°C. The etching time depended on the LET, the energy of the ions, and the desired size of the etched pits (also see below). For the experiments described here, the tracks from 10.2 MeV/nucleon carbon ions (preirradiation, see below) were etched for 15 min, and the tracks from the experimental 10.1 MeV/nucleon calcium ions were etched for 2 min.

Microscopy and Image Processing

Microscopy was done on a Leica DM/IRBE inverted microscope that was equipped with a Märzhäuser computerized stage control SCAN 100 × 100 and a 63× PlanApo lens. Video images (512 × 512 pixels) were captured using a standard black and white camera and a DT2851 (Data Translation) image acquisition board. Images were processed using the ScionImage (Scion Corporation, Frederick, MD) and ImageTool (University of Texas, San Antonio) programs. The software for the stage control was developed at GSI. Although the theoretical accuracy of the computerized stage is of the order of better than 1 μm, the actual accuracy is reduced significantly by the mechanical tolerance of the sample holder. The relocation procedure thus had to be improved by using two fiducial marks on each sample; these were produced by scratching tiny crosses in the CR39 plates using a scalpel. Rotational and translational displacements between subsequent observations of the same sample could then be detected. The overall repositioning accuracy was of the order of sev-

eral micrometers. This precision, however, was still not sufficient to investigate the correlation between particle tracks and CDKN1A foci.

Soyland and Hassfjell solved this problem by using internal reference marks that could be observed in the phase-contrast images because of the specific background patterns of the track etch material on which the cells were grown. However, we could not use this procedure, because the cells were grown as nearly confluent monolayers, and thus any background structure of the CR39 material was masked by the cell layer. Therefore, we produced artificial background structures by irradiating the CR39 plates at low fluences and then etching the plates before they were used to grow cells. By using appropriate etching times, the size of the track pits can be chosen so that they are clearly visible even in bright-field or phase-contrast illumination, without being masked by the cells. In the examples shown in the present analysis, the CR39 plates were preirradiated with a fluence of 1.4 × 10⁵ particles cm⁻² 10.2 MeV/nucleon carbon ions (LET 153 keV/μm) and latent tracks were etched for 15 min. For the 63× PlanApo lens, this fluence results in an average of 18 reference tracks per field of view (135 × 90 μm²). These preirradiated and etched CR39 plates were then sterilized using alcohol, washed in distilled water, and coated with CELL-TAK for use as the cell culture substratum. During the final analysis, the reference tracks and the tracks from the cell irradiation could be distinguished easily by their different sizes. The reference tracks were much larger because they had been etched for 15 min before the cells were plated and etched again during development of the tracks from the cell irradiation procedure (i.e. the 2-min etching for the 10.1 MeV/nucleon calcium ions).

Figure 1 shows the three different types of images necessary for the analysis. Figure 1a is a phase-contrast image in which the reference tracks produced by the preirradiation of the CR39 are clearly visible as bright spots. The rectangle indicates the position of a nucleus. Figure 1b shows the fluorescence image (type II) for this nucleus with CDKN1A localizing to discrete foci; the type I and II images were taken simultaneously without moving the sample. Figure 1c shows a phase-contrast image of the pattern of particle traversals after removal of the cells and etching of the latent tracks. The two groups of tracks can be identified unambiguously: The pattern of large bright tracks from preirradiation corresponds to the tracks already visible in Fig. 1a, whereas the small spots indicate the tracks produced by the cell irradiation procedure.

The shift of the images in Figs. 1a and b compared to Fig. 1c is due to the limited mechanical precision of the sample holder and the repositioning of the sample. However, the individual images can be matched precisely using the specific pattern of the reference tracks.

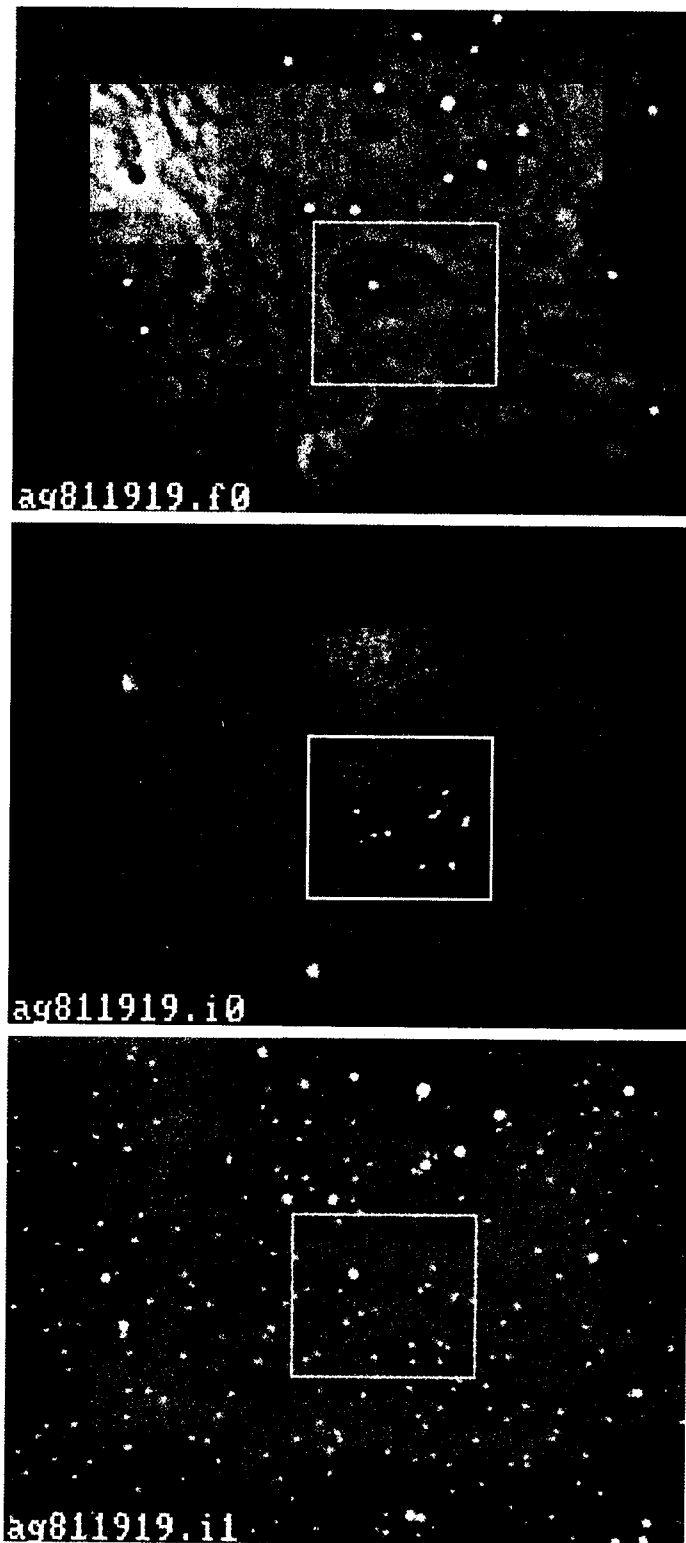
RESULTS

Figure 2 shows a representative example of the analysis to correlate the patterns of particle traversals and of CDKN1A foci, based on the images shown in Fig. 1. For clarity, these images were processed further to reduce the background and to make the specific patterns as clear as possible.

First, the type I images were transformed using a threshold procedure to specifically select only the reference track structures. Second, the type II images were optimized by adjusting the contrast manually. The corresponding images I/II were then combined using a false color coding, so that the reference tracks appeared in green, whereas the fluorescence intensity of the CDKN1A signal remained as a grayscale pattern (Fig. 2a). The type III images were also segmented according to a manually adjusted threshold, and the corresponding objects were subsequently classified into two groups according to their size. Again, the reference

tracks were color coded as green, while the tracks corresponding to the cell irradiation were coded in red.

To facilitate the comparison further, the important structures were indicated by light blue lines. The approximate



shape and size of the cell nuclei were represented by ellipses. Individual CDKN1A foci were interconnected by straight lines to enhance the particular pattern. The same pattern is shown in the lower panel (Fig. 2b) as an overlay to the track image. However, it was not drawn independently, but rather was obtained by a simple transfer of the pattern drawn in the top part of the figure. The line pattern copied from the fluorescence image matches the pattern of etched particle tracks exactly, and the patterns of CDKN1A foci and particle traversals coincide precisely.

A similar analysis was performed for about 20 fields in the sample that contained cells with clear CDKN1A signals; some examples of the resulting images are shown in Fig. 3. Only 1 or 2 nuclei per field of view, and in total approximately 35 cells of the 120 cells in all the fields analyzed, were found to show clear CDKN1A signals. This could be attributed to the fact that cells were not grown to full confluence. Our previous investigations suggest that it is probably the G_0/G_1 -phase cells that show distinct CDKN1A foci (1). The number of responding cells is expected to be significantly lower for the experimental conditions described here than it would be in confluent cultures.

In most of the examples shown in Fig. 3, there is a striking coincidence between the patterns of the fluorescent foci and of the etched tracks with respect to the relative structures and to their absolute positions compared to the reference marks. However, there were some cases in which the *absolute* position of the pattern of foci was shifted up to several micrometers. In these cases, the *relative* pattern matched the track pattern exactly. The relative translational displacement between the observed position of the foci and the position expected from the reference marks is indicated in Fig. 3b by the white arrows. In some cases, both a shift and a slight rotation ($<15^\circ$) had to be applied to achieve the maximum overlap between the different patterns. The shift and rotation could be due to either a technical problem (e.g. artifacts related to the detachment of cells during fixation and staining) or to cell movement during the 1-h interval between the irradiation and fixation of the sample. There was only one case out of 20 in which no agreement between the position of CDKN1A foci and the ion traversals could be detected.

DISCUSSION AND CONCLUSIONS

A precise correlation has been found between the patterns of particle traversals and of nuclear CDKN1A foci

←
FIG. 1. Comparison of the different types of images taken for the analysis. Upper panel: Phase-contrast image (type I) showing a cell nucleus and the reference tracks (bright spots) obtained by preirradiation and etching of the CR39 cell substratum. Middle panel: Fluorescence image (type II) at the same position, showing the distinct foci of the CDKN1A response within the cell nucleus. Lower panel: Phase-contrast image of tracks after removal of the cells and subsequent etching to detect the particle traversals from cell irradiation. Scale bar: 10 μm .

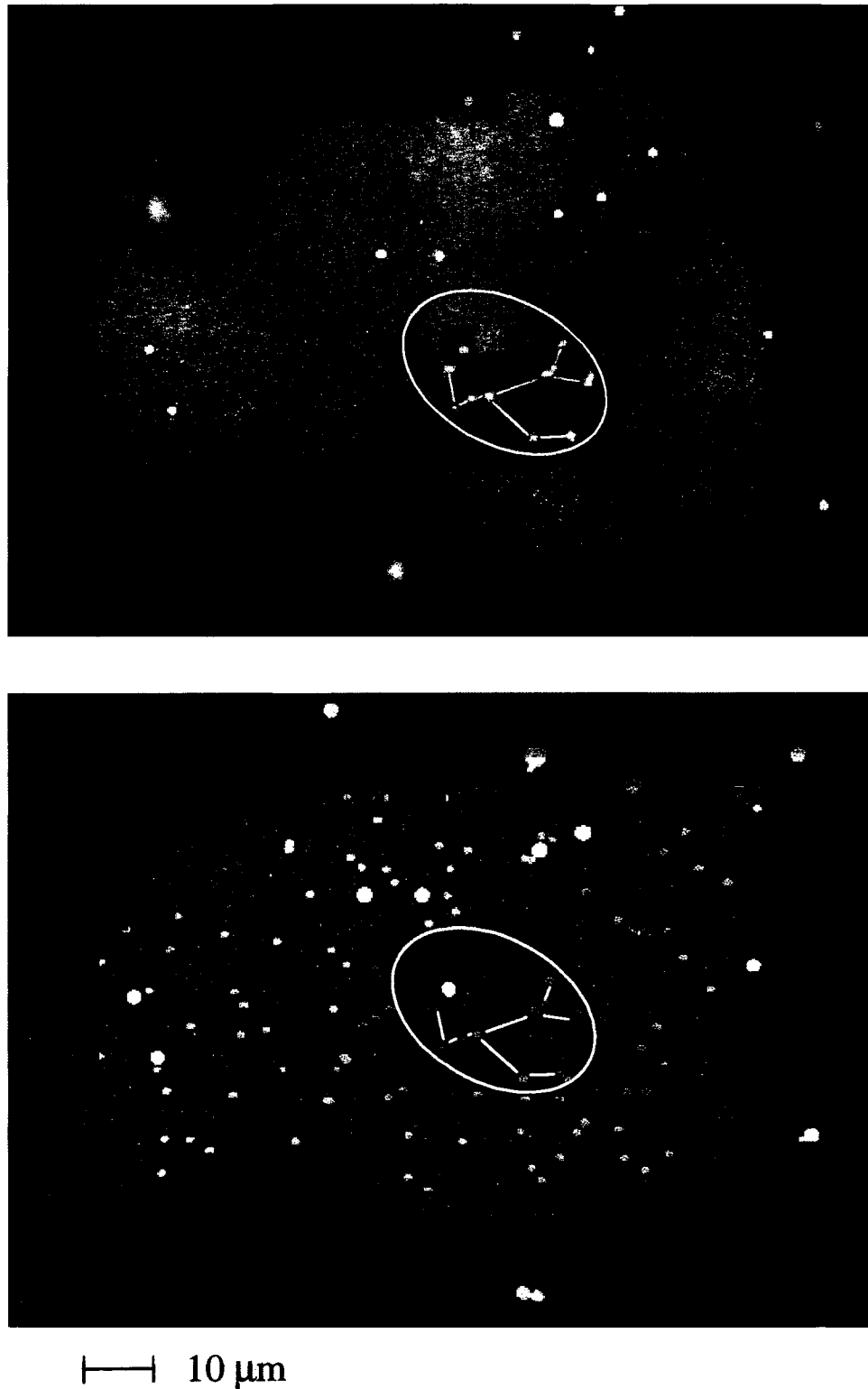
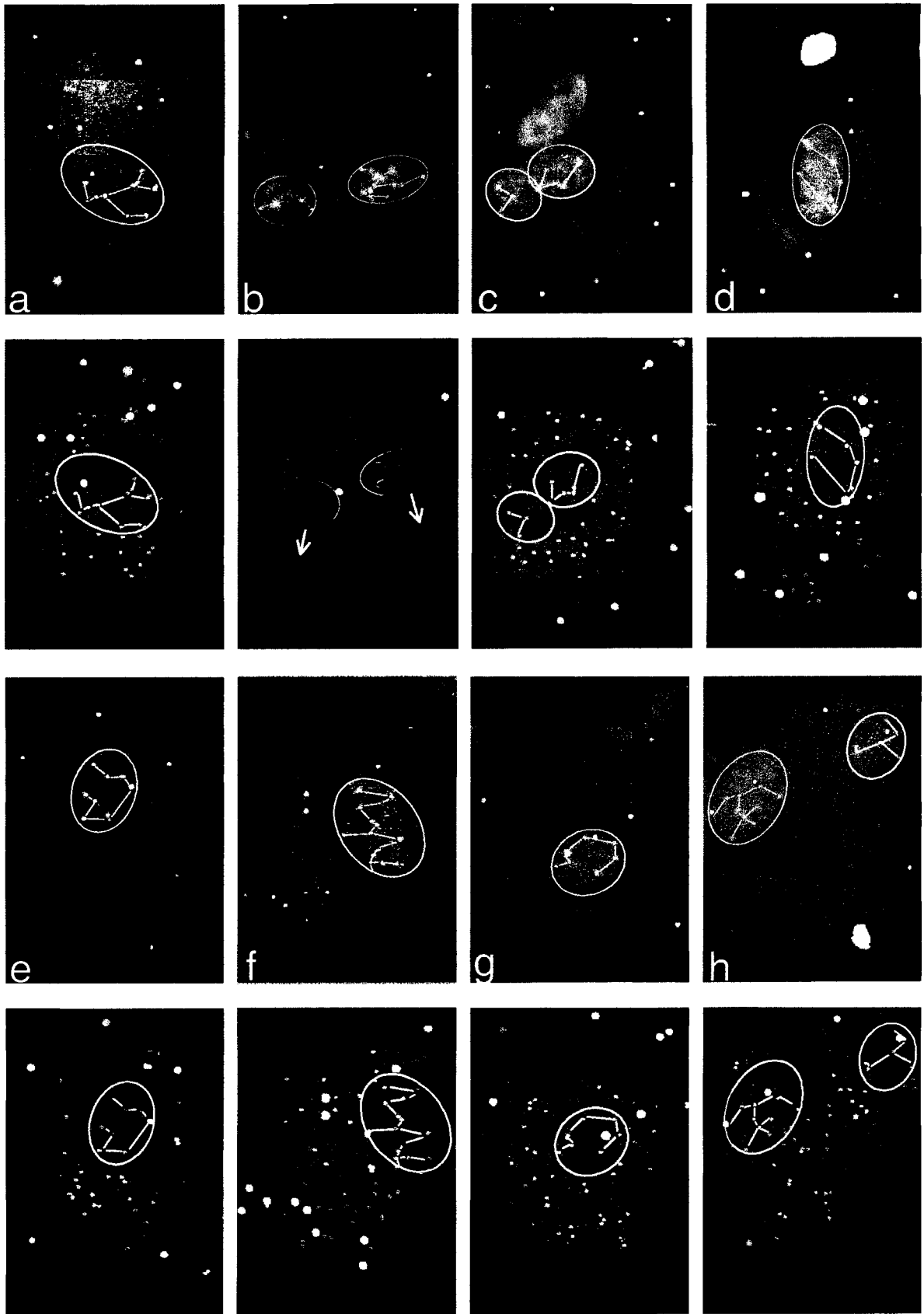


FIG. 2. Comparison of the pattern of CDKN1A foci with the pattern of particle traversals. Upper panel: Combined images type I and II, showing the reference tracks (green) and fluorescence intensity (grayscale). Lower panel: Segmented image type III, showing the reference tracks (green) and the particle traversals from cell irradiation (red). The light blue lines were drawn manually in the upper panel to indicate the size of the nucleus and the structure of the CDKN1A response pattern. The corresponding pattern in the lower panel is an exact copy of the pattern in the top panel. Scale bar: 10 μm .



10 μ m

induced by heavy-ion irradiation in human fibroblasts; in all but one case, the individual patterns could be clearly matched. The analysis thus represents the first direct evidence that individual CDKN1A foci can be attributed to individual particle traversals.

This spatial correlation is evident even in cases in which the particular pattern of CDKN1A foci is shifted for several micrometers with respect to the expected position, since it is highly improbable that such distinct patterns are produced just by chance. The reason for the observed shift remains unclear; it could be due to artifacts in the preparation of the sample as well as cell movements during the 1-h incubation after irradiation. However, preliminary investigations of cell motility indicate that displacements of the order of several micrometers per hour can be expected (data not shown), supporting the latter hypothesis. If this observation is confirmed, the stability of the CDKN1A pattern would indicate an extreme stability of the nuclear DNA organization for intervals of at least an hour, despite the significant movement of the cell. Similar findings that internal structures of the cell nucleus are highly conserved even during cell movement have been reported by Zink *et al.* (6). An extension of the studies reported here to longer times could thus provide a tool to study the nuclear reorganization of damaged sites after irradiation. Here, the changes in the relative positions of individual foci within a nucleus with respect to the pattern of particle traversals as well as the changes in the appearance of the foci would be of interest. The transition to a fuzzier appearance of CDKN1A foci at later times was reported in our previous study (1).

The data reported here present further evidence that CDKN1A binds to the sites of primary radiation-induced damage, although the function of CDKN1A for DNA damage recognition or processing remains to be clarified. Such a correlation with sites of damaged DNA is also supported by recent findings (7) proving the association of CDKN1A with DNA and showing the colocalization of foci with binding sites of the MRE11A/Rad50/NBS1 complex, which is known to be involved in the processing of DNA damage (8).

CDKN1A has recently been reported to be an appropriate indicator for use in investigations of bystander effects (9). However, the studies involving induction of CDKN1A were

based largely on statistical arguments related to the number and distribution of responding cells. The assignment of particle tracks to individual cells by the method presented here would enable us to distinguish primary damaged cells from secondary responding cells, and would thus represent an ideal tool to further elucidate the mechanisms of bystander effects.

ACKNOWLEDGMENT

We are thankful to G. Kraft for continuous support and encouragement and for suggestions to improve the manuscript.

Received: March 5, 2001; accepted: July 3, 2001

REFERENCES

1. B. Jakob, M. Scholz and G. Taucher-Scholz, Immediate localized CDKN1A (p21) radiation response after damage produced by heavy-ion tracks. *Radiat. Res.* **154**, 398–405 (2000).
2. C. Soyland and S. P. Hassfjell, A novel ^{210}Po -based α -particle irradiator for radiobiological experiments with retrospective α -particle hit per cell determination. *Radiat. Environ. Biophys.* **39**, 125–130 (2000).
3. C. Soyland, S. P. Hassfjell and H. B. Steen, A new alpha-particle irradiator with absolute dosimetric determination. *Radiat. Res.* **153**, 9–15 (2000).
4. M. Pugliese, M. Durante, G. F. Grossi, F. Monforti, D. Orlando, A. Ottolenghi, P. Scampoli and G. Gialanella, Inactivation of individual mammalian cells by single α -particles. *Int. J. Radiat. Biol.* **72**, 397–407 (1997).
5. G. Kraft, H. W. Daues, B. Fischer, U. Kopf, H. P. Liebold, D. Quis and H. Stelzer, Irradiation chamber and sample changer for biological samples. *Nucl. Instrum. Methods* **168**, 175–179 (1980).
6. D. Zink, T. Cremer, R. Saffrich, R. Fischer, M. F. Trendelenburg, W. Ansorge and E. H. K. Stelzer, Structure and dynamics of human interphase chromosome territories *in vivo*. *Hum. Genet.* **102**, 241–251 (1998).
7. B. Jakob, M. Scholz and G. Taucher-Scholz, Characterisation of CDKN1A (p21) binding to sites of heavy ion induced damage: Colocalisation with proteins involved in DNA repair. *Int. J. Radiat. Biol.*, in press.
8. R. S. Maser, K. J. Monsen, B. E. Nelms and J. H. Petrini, hMre11 and hRad50 nuclear foci are induced during the normal cellular response to DNA double-strand breaks. *Mol. Cell. Biol.* **17**, 6087–6096 (1997).
9. E. I. Azzam, S. M. de Toledo and J. B. Little, Direct evidence for the participation of gap junction-mediated intercellular communication in the transmission of damage signals from α -particle irradiated to nonirradiated cells. *Proc. Natl. Acad. Sci. USA* **98**, 473–478 (2001).

FIG. 3. Comparison of the pattern of CDKN1A foci with the pattern of particle traversals for different positions in the sample. For an explanation of the colors and lines, see the legend to Fig. 2. Scale bar: 10 μm . In panel b, the white arrows indicate the displacement of the observed CDKN1A pattern relative to the position expected from the track pattern.